arXiv:0907.3057v1 [physics.comp-ph] 17 Jul 2009

Conformational Mechanics of Polymer Adsorption Transitions at Attractive Substrates

Monika Möddel,* Michael Bachmann,† and Wolfhard Janke‡
Institut für Theoretische Physik, Universität Leipzig, Postfach 100 920, D-04009 Leipzig, and Centre for Theoretical Sciences (NTZ), Emil-Fuchs-Straße 1, D-04105 Leipzig, Germany

Conformational phases of a semiflexible off-lattice homopolymer model near an attractive substrate are investigated by means of multicanonical computer simulations. In our polymer-substrate model, nonbonded pairs of monomers as well as monomers and the substrate interact via attractive van der Waals forces. To characterize conformational phases of this hybrid system, we analyze thermal fluctuations of energetic and structural quantities, as well as adequate docking parameters. Introducing a solvent parameter related to the strength of the surface attraction, we construct and discuss the solubility-temperature phase diagram. Apart from the main phases of adsorbed and desorbed conformations, we identify several other phase transitions such as the freezing transition between energy-dominated crystalline low-temperature structures and globular entropy-dominated conformations.

I. INTRODUCTION

The study of the conformational behavior of polymers near surfaces is a fascinating field, both from a physical and chemical perspective. It provides a rewarding playground for basic and applied research. With the advent of new sophisticated experimental techniques offering an enormous potential in polymer and surface research, the interest in the hybrid interface of organic and inorganic matter has increased. Among such techniques at the nanometer scale is, for example, atomic force microscopy (AFM), where it is possible to measure the contour length and the end-to-end distance of individual polymers [1] or to quantitatively investigate the peptide adhesion on semiconductor surfaces [2]. Another experimental tool with an extraordinary resolution in positioning and accuracy in force measurements are optical tweezers [3, 4].

Applications for adsorption phenomena in polymeric solutions can be found in such different fields as lubrication, adhesion and surface protection, steric stabilization of colloidal particles, as well as in biological processes of membrane-polymer interaction. The understanding of the latter is particularly important for the reconstruction of cell processes. The knowledge of structure formation processes near interfaces is also a prerequisite for designing micro- or nanostructures providing a large variety of possible applications in nanotechnology.

Despite much efforts in the past, the solvent-quality-dependent behavior of a dilute polymer solution exposed to an adsorbing substrate is not yet fully understood. In good solvent, dominating structures are random coils since the monomers and the solvent molecules attract each other and, consequently, solvent molecules accumulate between monomers and push the monomers apart. Also at high temperatures, random coils are favored as they possess a higher conformational entropy than globular conformations. Reducing the temperature, the more compact low-energy conformations gain thermodynamic weight, and the polymer collapses in a cooperative rearrangement of the monomers. At the θ-temperature, where the self-avoidance effect and the solvent effect exactly cancel, the size of a flexible polymer scales like an ideal chain, that is, $\langle R_{\mathrm{gyr}}^2 \rangle \propto N^{2\nu}$, with $\nu = 1/2$. Globular conformations are highly compact but have only little internal structure. Hence those conformations are still entropy-dominated, and a further transition toward low-degenerate crystalline energetic states is expected and indeed observed: the freezing transition [5, 6].

The presence of an attractive surface strongly affects the behavior of the polymer in the vicinity of the interface. The monomer-monomer attraction, being responsible for the collapse below the θ-point, and the surface-monomer attraction, resulting in the adsorption, compete with each other. This competition gives rise to a variety of different conformational phases. The polymer adsorbs at the surface, if the temperature is decreased below the adsorption transition temperature, but at high temperatures only a small number of monomers is in contact with the surface, even if the polymer was grafted to it [7, 8]. This is due to the lower entropy of conformations spread out on the surface, compared to the behavior in bulk.

Numerous detailed studies have been performed to elucidate the conformational behavior of homopolymers and heteropolymers near substrates. Compared to experiments, computer simulations have the advantage that combinations of parameters can be varied at will. Theoretical studies have, for example, been performed analytically using scaling theory [9, 10], mean-field density functional theory [11], and series expansion [12, 13] and numerically by employing off-lattice models such as a bead-spring model of a single polymer chain grafted to a weakly attractive surface [8, 14], multiscale modelling [15], Monte Carlo studies of lattice homopolymers [7, 8, 9, 16, 17, 18, 19, 20, 21], molecular dynamics combined with a stretching of an adsorbed

*E-mail: Monika.Moeddel@itp.uni-leipzig.de
†E-mail: Michael.Bachmann@itp.uni-leipzig.de
‡E-mail: Wolfhard.Janke@itp.uni-leipzig.de;
Homepage: http://www.physik.uni-leipzig.de/CQT.html

homopolymer [22], or exact enumeration [23]. Also adsorption-desorption dynamics were investigated in Brownian dynamics simulations of coarse-grained models [24].

In this study, we performed multicanonical Monte Carlo computer simulations in order to analyze thermodynamic properties of the adsorption of a semiflexible polymer at a flat and unstructured, attractive substrate. Our main objective is the classification of the structural phases accompanying the adsorption process and the construction of the complete (pseudo)phase diagram parametrized by the temperature and a suitably introduced solvent-quality parameter. The rest of the paper is organized as follows. In Sect. II, the hybrid polymer-substrate model, the multicanonical simulation method, as well as the measured observables are introduced. The main result, the pseudophase diagram, is presented and discussed in detail in Sect. III. Several aspects of the phase structure are consolidated by a precise analysis of individual observables introduced in Sect. II. In Sect. IV, our off-lattice results are compared with former results obtained in simulations of lattice models. Eventually, in Sect. V, the paper is concluded by a summary of our findings.

II. THE MODEL

A. Hybrid Modeling of Polymer-Substrate Interaction.

We employ a coarse-grained off-lattice model for semiflexible homopolymers that has also been generalized for studies of heteropolymers [25, 26] and helped to understand protein folding channels from a mesoscopic perspective [27, 28]. In contrast to earlier adsorption studies of lattice polymers [7, 8, 9, 16, 17, 18, 19, 20, 21], we here accept the associated additional computational cost of an off-lattice model in order to get rid of undesired effects of underlying lattice symmetries.

As on the lattice, we assume that adjacent monomers are connected by rigid covalent bonds. Thus, the distance $|\vec{r}_{i+1} - \vec{r}_i|$ is fixed and set to unity. Bond and torsional angles are free to rotate. The energy function consists of three terms,

$$E = E_{\rm bend} + E_{\rm LJ} + E_{\rm sur} \tag{1}$$

associated with the bending stiffness ($E_{\rm bend}$), monomer-monomer Lennard-Jones interaction ($E_{\rm LJ}$), and monomer-surface attraction ($E_{\rm sur}$).

A sketch of a coarse-grained polymer segment is depicted in Figure 1. The position vector of the ith monomer, $i = 1, \ldots, N$, is denoted by $\vec{r}_i$. A polymer with N monomers has $N-1$ bonds of length unity between neighboring monomers and $N-2$ bending angles ϑ_i, $i = 1, \ldots, N-2$, defined through

$$\cos(\vartheta_i) = (\vec{r}_{i+1} - \vec{r}_i) \cdot (\vec{r}_{i+2} - \vec{r}_{i+1}) \,. \tag{2}$$

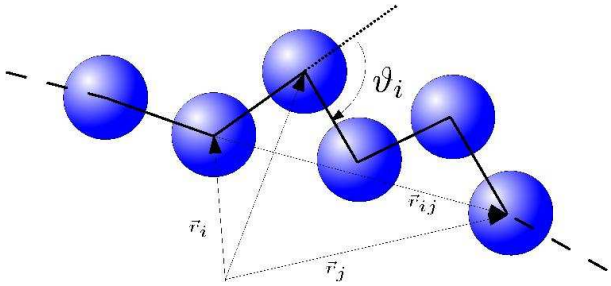

FIG. 1: A segment of the coarse-grained semiflexible polymer. The distance between two adjacent monomers is fixed and set to unity. The bending angle at the $(i+1)$th monomer is denoted by ϑ_i, and the vector between the ith and jth monomer by $\vec{r}_{ij} \equiv \vec{r}_j - \vec{r}_i$ with $|\vec{r}_{ij}| = r_{ij}$.

The Lennard-Jones potential of nonbonded monomers is of standard form,

$$E_{\rm LJ} = 4 \sum_{i=1}^{N-2} \sum_{j=i+2}^{N} \left(\frac{1}{r_{ij}^{12}} - \frac{1}{r_{ij}^{6}} \right), \tag{3}$$

where $r_{ij} = |\vec{r}_j - \vec{r}_i|$. The lowest-energy distance of the Lennard-Jones potential between two monomers is $r_{\rm min} = \sqrt[6]{2} \approx 1.12$ and is hence slightly larger than the unity bond length. The bending energy is defined as

$$E_{\rm bend} = \frac{1}{4} \sum_{i=1}^{N-2} \left(1 - \cos(\vartheta_i)\right). \tag{4}$$

The angle ϑ_i is in the interval $[0, \pi)$ and the bending energy can be considered as a penalty for successive bonds deviating from a straight arrangement.

The attractive surface potential is obtained by integrating over a smooth half-space, where every space element interacts with a single monomer by the usual Lennard-Jones 12-6 expression. One obtains the potential [29, 30]:

$$E_{\rm sur} = \epsilon_s \sum_{i=1}^{N} \left[\frac{2}{15} \left(\frac{1}{z_i} \right)^9 - \left(\frac{1}{z_i} \right)^3 \right], \tag{5}$$

where z_i is the distance of the ith monomer from the surface. The parameter ϵ_s defines the surface attraction strength, and as such it weighs the energy scales of intrinsic monomer-monomer attraction and monomer-surface attraction.

A distance $z = L_{\rm box}$ away from the attractive surface, we place a steric wall that is necessary to prevent the molecule from escaping. Because the exact form of the density of states depends on the box height $L_{\rm box}$, all measured quantities also depend on the choice of $L_{\rm box}$. As soon as the box size exceeds the polymer size, however, the influence on the observables, apart from the substrate distance of the center-of-mass $z_{\rm cm} = \sum_{i=1}^{N} z_i/N$ of the polymer, is sufficiently small. We chose $L_{\rm box} = 20\,(40)$ for the polymer with $N = 13\,(20)$ monomers.

B. Multicanonical Method.

The canonical partition function of our hybrid system at temperature T is given in natural units by

$$Z = \int_{E_{\min}}^{\infty} \mathrm{d}E\, g(E) \mathrm{e}^{-E/T}, \tag{6}$$

where $g(E) = \mathrm{e}^{S(E)}$ is the density of states that connects (microcanonical) entropy S and energy. Therefore, all information regarding the phase behavior of the system – typically governed by the competition between entropy and energy – is encoded in $g(E)$. Consequently, for a detailed global analysis of the phase behavior, a precisely estimated density of states is extremely helpful. Unfortunately, the density of states covers many orders of magnitude in the phase transition regimes, so that its estimation requires the application of sophisticated generalized-ensemble Monte-Carlo methods.

For our analyses, we have performed multicanonical simulations [31], as multicanonical sampling allows the estimation of $g(E)$, in principle, within a single simulation. The idea of the multicanonical method is to increase the sampling rate of conformations being little favored in the free-energy landscape and, finally, to perform a random walk in energy space. This is achieved in the simplest way by setting $T = \infty$ and introducing suitable multicanonical weights $W_{\mathrm{muca}}(E) \sim g^{-1}(E)$ in order to sample conformations $\mathbf{X}$ according to a transition probability

$$\omega(\mathbf{X} \to \mathbf{X}') = \min[\mathrm{e}^{S(E(\mathbf{X}))-S(E(\mathbf{X}'))}, 1], \tag{7}$$

where $S(E(\mathbf{X})) = -\ln W_{\mathrm{muca}}(E(\mathbf{X})) = \ln g(E(\mathbf{X}))$.

The implementation of multicanonical sampling is not straightforward as the multicanonical weights $W_{\mathrm{muca}}(E)$ are obviously unknown a priori. Therefore, starting with $W^0_{\mathrm{muca}}(E) = \text{const.}$, the weights have to be determinded by an iterative procedure until the multicanonical histogram is almost "flat", that is, if the estimate for the density of states after the nth run, $\hat{g}^{(n)}(E)$, satisfies

$$\hat{g}^{(n)}(E) W^{n-1}_{\mathrm{muca}}(E) \approx \text{const.} \tag{8}$$

in the desired range of energies. An efficient, error-weighted estimation method for the multicanonical weights is described in detail in refs [32] and [33].

Eventually, if eq 8 is reasonably satisfied, the multicanonical weights $W^n_{\mathrm{muca}}(E) = [\hat{g}^{(n)}(E)]^{-1}$ are then used in a final long production run, where all quantities of interest are measured and stored in a time-series file. The canonical expectation value of any quantity O at temperature T is then obtained from the multicanonical time series of length M by reweighting,

$$\langle O \rangle = \frac{\sum_{i=1}^{M} O(\mathbf{X}_t) \mathrm{e}^{-E(\mathbf{X}_t)/T} W^{-1}_{\mathrm{muca}}(E(\mathbf{X}_t))}{\sum_{i=1}^{M} \mathrm{e}^{-E(\mathbf{X}_t)/T} W^{-1}_{\mathrm{muca}}(E(\mathbf{X}_t))}, \tag{9}$$

where t is the multicanonical Monte Carlo "time" step (or sweep).

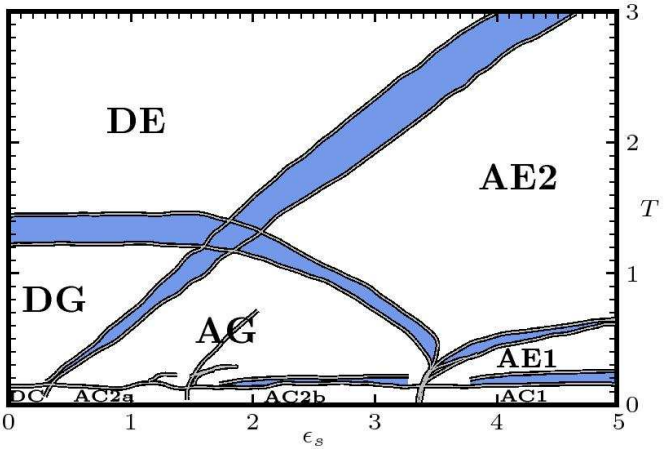

FIG. 2: Phase diagram of the 20mer. The colored stripes separate the individual conformational phases (see text and Figure 3).

C. Suitable Energetic and Structural Quantities for Phase Characterization.

To obtain as much information as possible about the canonical equilibrium behavior, we define the following suitable quantities O. Next to the canonical expectation values $\langle O \rangle$, we also determine the fluctuations about these averages, as represented by the temperature derivative $(\langle OE \rangle - \langle O \rangle \langle E \rangle)/T^2$. We use generic units, in which $k_B = 1$.

Apart from energetic fluctuations such as the specific heat, $c_V = \mathrm{d}\langle E/N \rangle \mathrm{d}T$, several structural quantities are of interest. The radius of gyration is a measure for the extension of the polymer and defined by $R^2_{\mathrm{gyr}} \equiv \sum_{i=1}^{N} \langle (\vec{r}_i - \vec{R}_{\mathrm{cm}})^2 \rangle / N = \sum_{i=1}^{N} \sum_{j=1}^{N} \langle (\vec{r}_i - \vec{r}_j)^2 \rangle / 2N^2$ with $\vec{R}_{\mathrm{cm}} = \sum_{i=1}^{N} \vec{r}_i / N$ being the center-of-mass of the polymer. Since the substrate introduces a structural anisotropy into the system, it is not only useful to investigate the overall compactness of the polymer expressed by $\langle R_{\mathrm{gyr}} \rangle$, but also to study the expected different behavior of its components parallel and perpendicular to the surface: $R^2_{\parallel} = \sum_{i=1}^{N} \sum_{j=1}^{N} \langle (x_i - x_j)^2 + (y_i - y_j)^2 \rangle / 2N^2$ and $R^2_{\perp} = \sum_{i=1}^{N} \sum_{j=1}^{N} \langle (z_i - z_j)^2 \rangle / 2N^2$ such that $R^2_{\mathrm{gyr}} = R^2_{\parallel} + R^2_{\perp}$.

Clear evidence that the polymer is, on average, freely moving in the box or very close to the surface can be provided by the distance of the center-of-mass, z_{cm}, of the polymer to the surface.

Another useful quantity is the mean number of monomers docked to the surface. A single-layer structure is formed if all monomers are attached at the substrate; if none is attached, the polymer is quasifree (desorbed) in solvent. The surface potential is a continuous potential, and in order to distinguish monomers docked to the substrate from those not being docked, it is reasonable to introduce a cutoff. We define a monomer i as being

pseudophase	typical configuration
DE	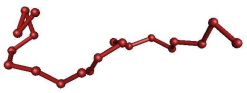
DG	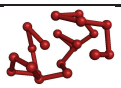
DC	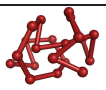
AE1	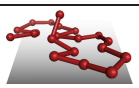
AE2	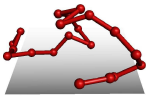
AC1	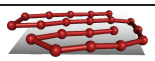
AG	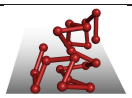
AC2a	
AC2b	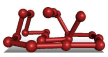

FIG. 3: Representative examples of conformations for the 20mer in the different regions of the T-ϵ_s pseudophase diagram. DE, DG, and DC represent bulk "phases", where the polymer in preferably desorbed. In regions AE1, AE2, AC1, AG, AC2a, and AC2b, conformations are favorably adsorbed.

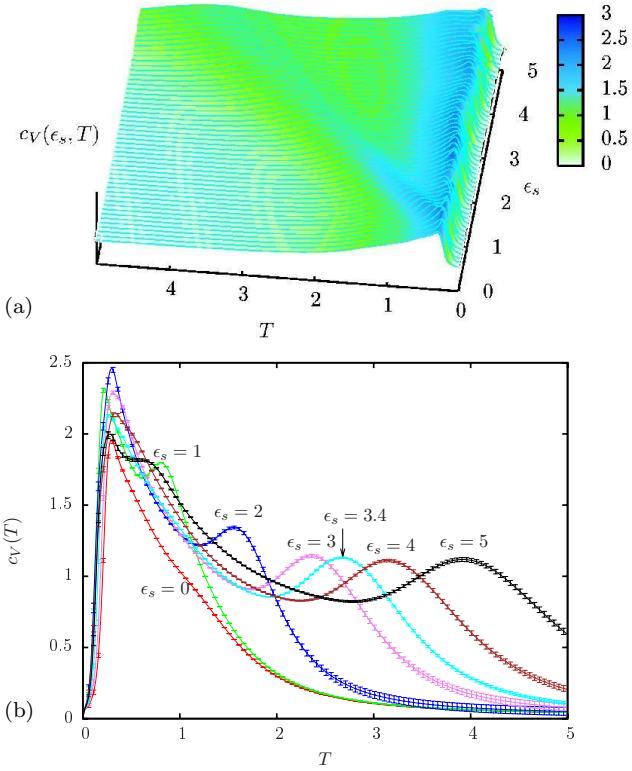

FIG. 4: (a) Specific heat as a function of temperature T and surface interaction strength ϵ_s for the 20mer. Lines represent the simulation data for fixed values of ϵ_s, the color code is interpolated. (b) Specific heat curves for different values of ϵ_s.

"docked" if $z_i < z_c \equiv 1.2$. The corresponding measured quantity is the average ratio $\langle n_s \rangle$ of monomers docked to the surface and the total number of monomers. This can be expressed as $n_s = N_s/N$ with $N_s = \sum_{i=1}^{N} \Theta(z_c - z_i)$, where $\Theta(z)$ is the Heaviside step function.

Similary, the mean number of intrinsic contacts is introduced as a measure of the global compactness of the polymer: $n_m = N_m/N$ with $N_m = \sum_{i=1}^{N-2} \sum_{j=i+2}^{N} \Theta\left(e_c - e_{\mathrm{LJ}}\left(r_{ij}\right)\right)$, where $e_c \equiv -0.2$ and $e_{\mathrm{LJ}}\left(r_{ij}\right) = 4\left(r_{ij}^{-12} - r_{ij}^{-6}\right)$.

III. RESULTS AND DISCUSSION

Our major objective is the construction of the pseudophase diagram of conformational phases, based on our results obtained for energetic and structural fluctuations. To this end, multicanonical simulations [31] for 51 different surface attraction strengths ϵ_s, in the range $\epsilon_s = 0, \ldots, 5$, were performed and reweighted to temperatures $T \in (0, 5]$. Each simulation consisted of 10^8 sweeps and was performed with at least 2 different initializations of the random number generator in order to avoid systematic deviations.

For a convenient overview, we display our final pseudophase diagram of the 20mer already here in Fig. 2. Conformations representative of the different phases are shown in Fig. 3. The details will be discussed in the following. It should be stressed that all phases and transitions occuring in our analysis are not phases in the strict thermodynamic sense, since we are dealing with finite chain lengths. However, even for the rather short chains considered here, a reasonable picture of the polymer adsorption behavior at the surface is obtained, and most of the phases are believed to still exist for longer chains.

A. Energetic Fluctuations

In Fig. 4(a), the specific heat of the 20mer is shown as a function of T and ϵ_s. Although for both investigated polymer lengths the energy varies smoothly with changing T and ϵ_s (with a global minimum at minimal temperature and maximal surface attraction), two transitions can be identified as ridges in the profile of the specific heat: The first one is the *adsorption transition*

separating desorbed and adsorbed conformations. The other transition is sort of a *freezing transition* at low temperatures. Near $T = 0.25$, the specific heat exhibits a pronounced peak and decreases rapidly at lower temperatures, independently of the surface attraction strength. The low-temperature peak in specific heat and the crystalline shape of structures found in this regime signalize this freezing transition. Although the freezing temperature seems to be rather constant, the type of crystalline structure adopted by the polymer depends strongly on ϵ_s. For the identification of the polymer shapes, we take in the next subsection a closer look at the conformational quantities.

B. Comparative Discussion of Structural Fluctuations

The radius of gyration provides an excellent measure of the globular compactness of polymer conformations. Figures 5 and 6 reveal that the most compact conformations dominate at low temperatures and for small values of surface attraction strengths ϵ_s. The freezing transition can be found at the same temperature, as it has already been identified from the specific heat. The adsorption transition typically affects only segments of the polymer and is thus not prominently signaled by the radius of gyration.

This is different for its components parallel (Figures 7 and 8) and perpendicular (Figures 9 and 10) to the surface, respectively. For example, for $\epsilon_s \geq 3.4$, $\langle R_\perp \rangle$ vanishes at low temperatures for the 20mer, whereas $\langle R_\parallel \rangle$ attains low values at lower ϵ_s. The vanishing of $\langle R_\perp \rangle$ corresponds to conformations where the polymer is spread out flat on the surface without any extension into the third dimension. The associated pseudophases are called adsorbed compact (AC1) and adsorbed expanded (AE1) phase. The '1' is appended in order to distinguish these phases from topological three-dimensional phases, such as, for example, the AC2 subphases. The phases AC1 and AE1 are separated by the freezing transition such that polymer structures in AC1 are maximally compact at lower temperatures, whereas AE1 conformations are less compact and more flexible but still lie rather planar at the surface. To verify that conformations in AC1 are indeed maximally compact single layers, we argue as follows. The most compact shape in the two-dimensional (2D) continuous space is the circular disk. Thus, one can calculate $\langle R_\parallel \rangle$ for a disk and compare it with the simulated value. Assuming N monomers to be distributed evenly in the disk, $N \approx \pi r^2$, where r is the radius of the disk in units of the mean distance of neighboring monomers. The radius of gyration in the same units is thus given by

$$R_{\mathrm{gyr,disk}}{}^2 = \frac{1}{\pi r^2} \int_{r' \leq r} \mathrm{d}^2 r' r'^2 = \frac{1}{2} r^2 \approx \frac{N}{2\pi}. \qquad (10)$$

Since we have two types of mean distances between

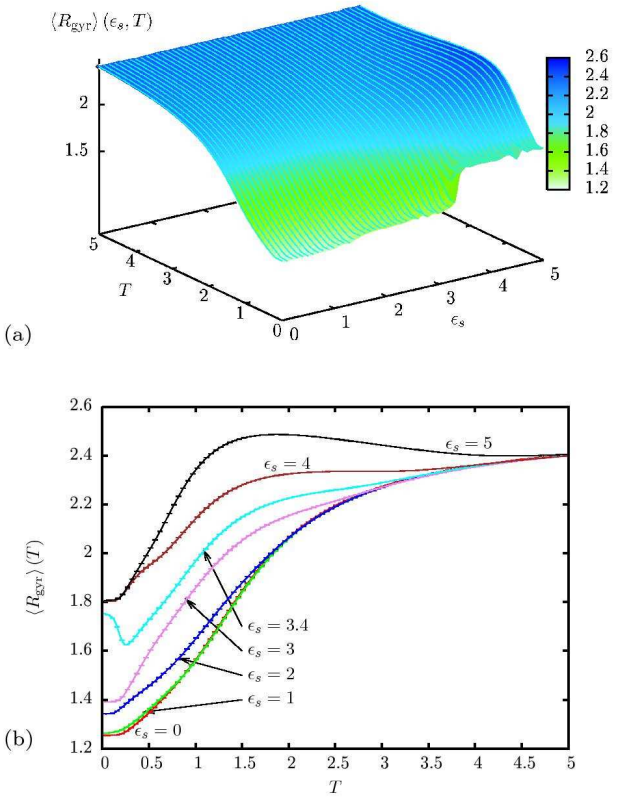

FIG. 5: (a) $\langle R_{\mathrm{gyr}} \rangle$ of the 20mer as a function of T and ϵ_s. (b) $\langle R_{\mathrm{gyr}} \rangle$ as a function of the temperature for various values of ϵ_s.

monomers in compact conformations dependent on whether they are adjacent along the chain or not, we expect for disk-like conformations an the surface: $\sqrt{20/2\pi} \approx 1.784 < \langle R_{\parallel,20} \rangle < 2.003 \approx r_{\min}\sqrt{20/2\pi}$. The simulated value is $\langle R_{\parallel,20} \rangle \approx 1.81$, which nicely fits the estimate. The equivalent estimate for the 13mer also confirms discoidal conformations in AC1.

The argument is similar for sphere-like three-dimensional (3D) compact conformations with $N = 4\pi r^3/3$. Corresponding conformations are found as free desorbed compact chains (DC), as well as adsorbed compact polymer conformations (AC2a) for weak surface attraction. In this case, the radius of gyration is given by

$$R_{\mathrm{gyr,sph}}{}^2 = \frac{1}{4\pi r^3/3} \int_{r' \leq r} \mathrm{d}^3 r' r'^2 = \frac{3}{5} r^2 \approx \frac{3}{5} \left(\frac{3N}{4\pi} \right)^{2/3}. \qquad (11)$$

The estimates $(3/5)^{1/2}(3 \times 13/4\pi)^{1/3} \approx 1.130 < \langle R_{\mathrm{gyr},13} \rangle < 1.268 \approx r_{\min}(3/5)^{1/2}(3 \times 13/4\pi)^{1/3}$, and $1.684 < \langle R_{\mathrm{gyr},20} \rangle < 1.464$ slightly overestimate the simulated values $\langle R_{\mathrm{gyr},13} \rangle = 1.023$ and $\langle R_{\mathrm{gyr},20} \rangle = 1.242$. The deviations can be explained by the fact that the mass of the polymer is not uniformly distributed in the sphere as it is assumed in the calculation. For a compact packing of discrete monomer positions, it is more realistic that

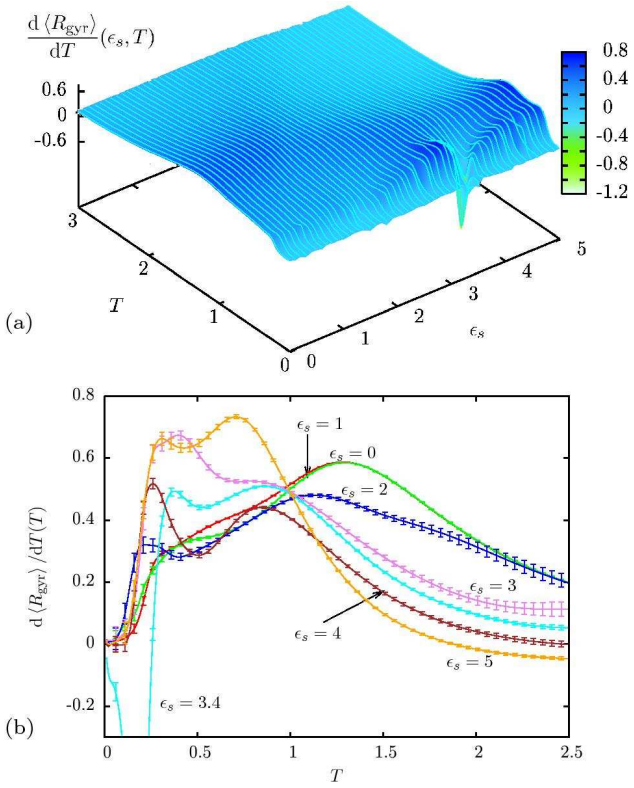

FIG. 6: (a) $\mathrm{d}\langle R_{\mathrm{gyr}}\rangle/\mathrm{d}T$ of the 20mer. (b) $\mathrm{d}\langle R_{\mathrm{gyr}}\rangle/\mathrm{d}T$, parametrized by ϵ_s.

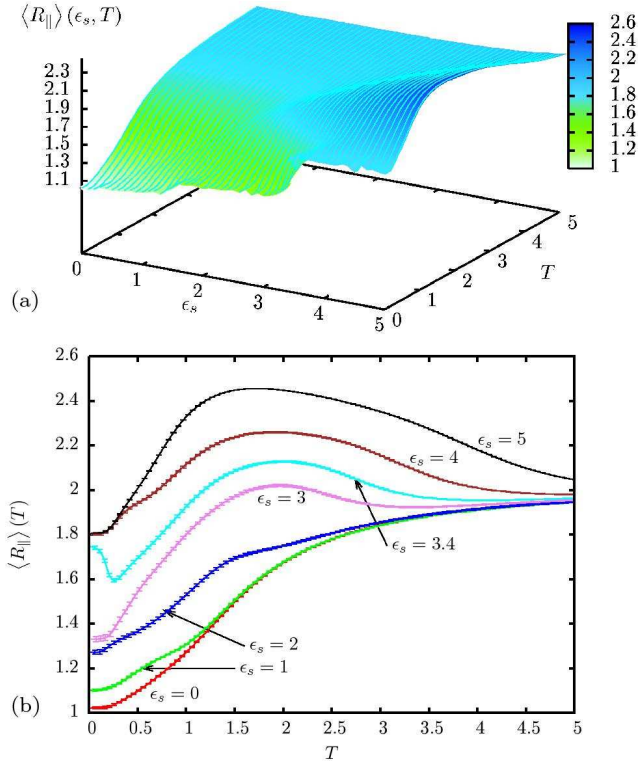

FIG. 7: (a) $\langle R_{\parallel}\rangle$ of the 20mer. (b) $\langle R_{\parallel}\rangle$ for selected values of ϵ_s.

the outer thin shell of the sphere does not contain any monomers. Performing the integration not from $r' = 0$ to $r' = r$, but only to $r' = r - \varepsilon$, reduces the estimated radius of gyration significantly already for small ε due to the increased weight of the outer shells in higher dimensions. Taking this effect into account, the thus obtained values of $\langle R_{\mathrm{gyr}}\rangle$ seem to be even more reasonable.

The most pronounced transition is the strong layering transition at $\epsilon_s \approx 3.4$ for $N = 20$ that separates regions of planar conformations (AC1, AE1) in the T-ϵ_s plane from the region of stable double-layer structures (AC2b) and adsorbed globules (AG), below and above the freezing transition, respectively. For high surface attraction strengths ϵ_s, it is energetically favorable to form as many surface contacts as possible. In the layering-transition region, a higher number of monomer-monomer contacts causes the double-layer structures to have just the same energy as single-layer structures. For lower ϵ_s values, the double-layer structures possess the lowest energies. Hence this transition is a sharp energetical transition.

Although for the considered short chains no higher-layer structures are observed, the components $\langle R_{\parallel,\perp}\rangle$ indicate some activity for low surface attraction strengths. For $N = 20$, $\epsilon_s \approx 1.4$ is the lowest attraction strength, where still stable double-layer conformations are found below the freezing transition. What follows for lower ϵ_s values after a seemingly continuous transition is a low-temperature subphase of surface attached compact con-

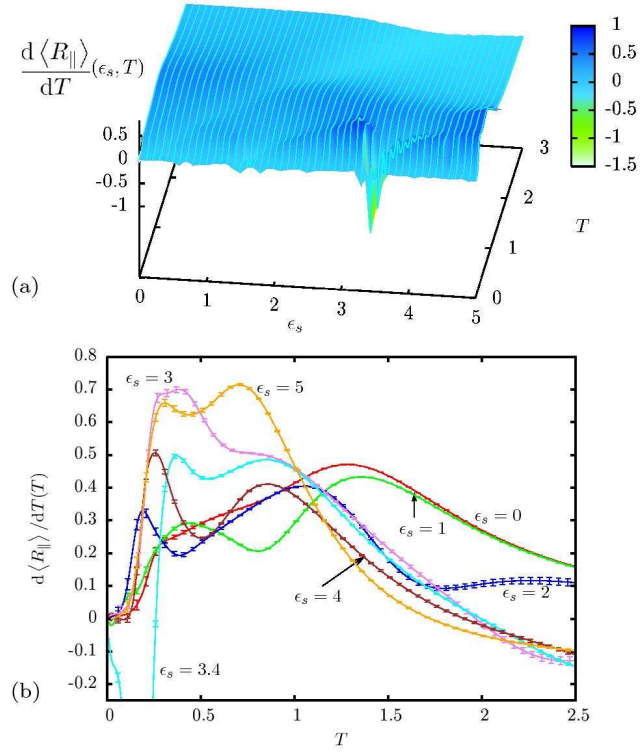

FIG. 8: (a) $\mathrm{d}\langle R_{\parallel}\rangle/\mathrm{d}T$ for the 20mer. (b) $\mathrm{d}\langle R_{\parallel}\rangle/\mathrm{d}T$ for different surface attraction strengths ϵ_s.

formations, called AC2a. AC2a conformations occur if the monomer-surface attraction is not strong enough to induce a layering in compact attached structures. The characterization of structures in this subphase requires some care, as system-size effects are dominant. Although the surface attraction is sufficiently strong to enable polymer-substrate contacts, compact desorbed polymer conformations below the θ-transition are not expected to change much. Thus, layering effects do not occur. We found two distinct classes of structures in this region: (1) completely undistorted compact conformations touching the surface and (2) semispherically shaped structures docked at the surface. For the rather short chains in our study, the occurrence of these shapes strongly depends on the precise number of monomers. Not surprisingly, we find differences for the 13mer and the 20mer.

For $N = 13$, both components of the radius of gyration, $\mathrm{d}\langle R_\perp\rangle/\mathrm{d}T$ and $\mathrm{d}\langle R_\parallel\rangle/\mathrm{d}T$, indicate a transition at $\epsilon_s \approx 0.45$. Low-energy configurations reveal that this is a wetting transition between undistorted compact conformations for smaller ϵ_s and docked conformations for largerr surface attraction strengths. An analogous transition for $N = 20$ was not found. In this case, the AC2a pseudophase seems to consist of a mixture of both types without any transition between them. This is also confirmed by analyzing the low-energy conformations in this regime. The higher the ϵ_s value, the larger the average number of monomers being docked at the surface, but a clear cut from the compact adsorbed conformations does not exist. This difference in the wetting transition for $N = 13$ and $N = 20$ might be due to the fact that the most compact conformation for $N = 13$ is an almost perfect icosahedron [34]. "Almost" because the length scales of covalent bonds and intermonomeric Lennard-Jones interaction differ slightly.

We also searched for low-energy states with a modified LJ energy minimum distance shifted to unity and indeed found perfectly icosahedral morphologies. This additionally stabilizes the polymer conformation and is already known from studies of atomic clusters. The smallest Mackay icosahedron [35] with characteristic 5-fold symmetry is formed by 13 atoms. Larger perfect icosahedra also require a "magic" number (55, 147, 309,...) of atoms. This holds also true for crystals of elastic polymers[34]. Thus, it might be worthwhile to also study the wetting transition for other chain lengths in order to be able to predict a trend for longer chains, which is not possible only knowing the behavior for the two chain lengths investigated in our study. The parameters of the low-temperatures pseudophase transitions for the 13mer and the 20mer are summarized in Table I.

Raising the temperature above the freezing temperature, polymers from adsorbed and rather compact conformations that look like glocular, unstructured drops on the surface. This pseudophase is called a *surface-attached globule* (AG) phase. It has been first conjectured from

TABLE I: Surface Attraction Strength ϵ_s for all Low-temperature Transitions for $N = 13$ and $N = 20$

transition	$N = 13$	$N = 20$
adsorption transition	$\epsilon_s \approx 0.2$	$\epsilon_s \approx 0.2$
transition AC $\leftrightarrow$ AC2a	$\epsilon_s \approx 0.5$	–
transition AC2a $\leftrightarrow$ AC2b	$\epsilon_s \approx 0.9$	$\epsilon_s \approx 1.7$
layering transition AC2b $\leftrightarrow$ AC1	$\epsilon_s \approx 2.8$	$\epsilon_s \approx 3.4$

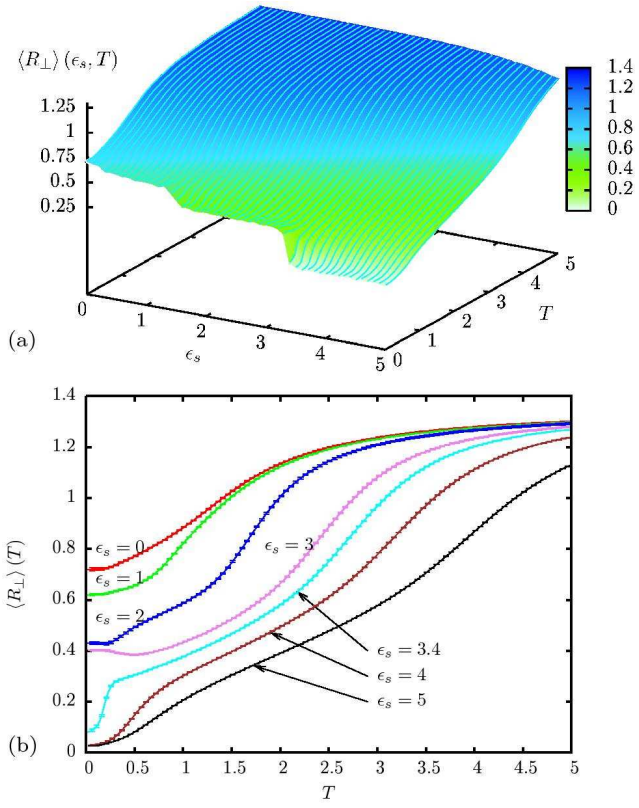

FIG. 9: (a) $\langle R_\perp\rangle$ of the 20mer. (b) $\langle R_\perp\rangle$ for selected values of ϵ_s.

short exact enumeration studies of 2D polymers in poor solvent [23] but was also found in lattice-polymer studies [7, 16]. At even higher temperatures, two scenarios can be distinguished in dependence of the relative strengths of monomer-monomer and monomer-substrate interactions. In the first case, the polymer first desorbs from the surface [from AG to the desorbed globular (DG) bulk phase] and disentangles at even higher temperatures [from DG to the desorbed expanded bulk phase (DE)]. In the latter case, the polymer expands while it is still on the surface (from AG to AE2) and desorbs at higher temperatures (from AE2 to DE). Due to the higher relative number of monomer-monomer contacts in compact bulk conformations of longer chains, the θ-temperature increases with N. The same holds true for the surface attraction strength, ϵ_s, associated with the layering transition.

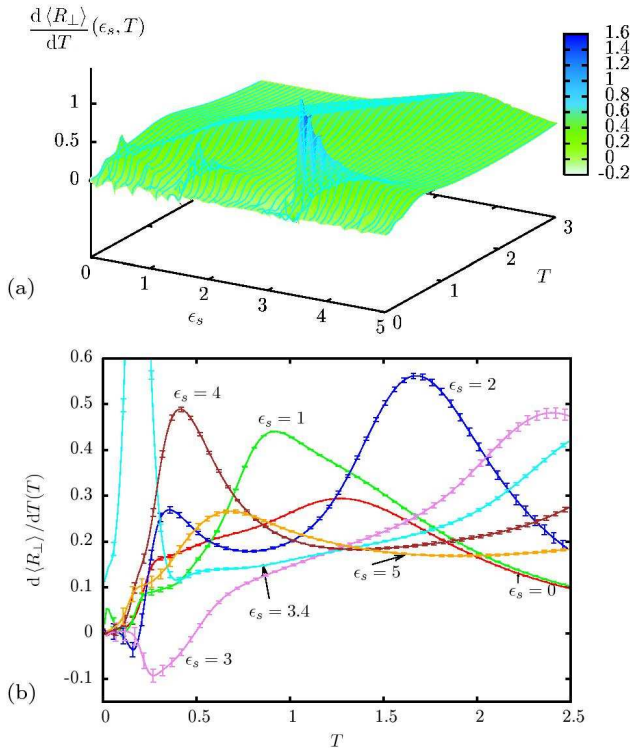

FIG. 10: (a) $\mathrm{d}\langle R_\perp\rangle/\mathrm{d}T$ of the 20mer. (b) $\mathrm{d}\langle R_\perp\rangle/\mathrm{d}T$ for different surface attraction strengths ϵ_s.

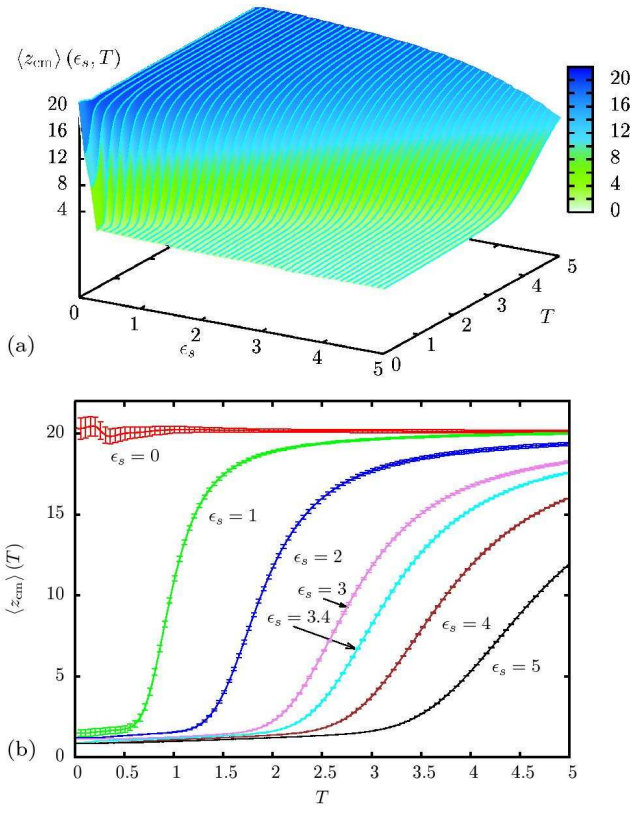

FIG. 11: (a) $\langle z_{\mathrm{cm}}\rangle$ of the 20mer. (b) $\langle z_{\mathrm{cm}}\rangle$ for various values of the parameter ϵ_s.

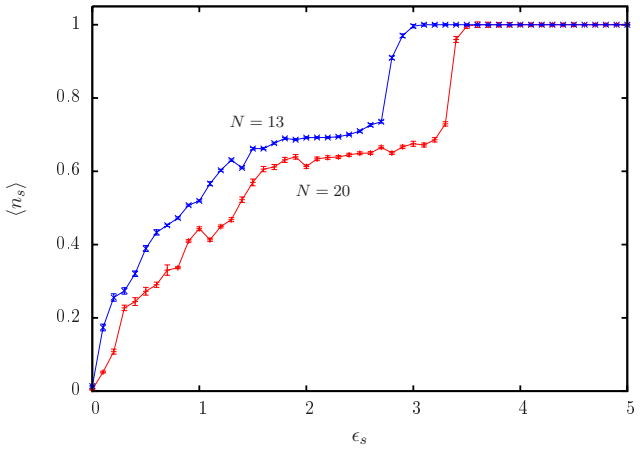

FIG. 12: Mean number of surface contacts $\langle n_s\rangle$ vs. surface attraction strength ϵ_s for the 13mer and the 20mer at $T = 0.001$.

It is clear that the structural behavior of the studied small chains is affected by finite-size effects, in particular in the compact pseudophases. As long as surface effects are as influential as volume effects, the shapes of compact adsorbed (but also of compact desorbed[34]) conformations differ noticeably for polymers with different but small lengths, and a precise classification is difficult. However, for longer chains, filmlike (AC1) and semispherical conformations (AC2), as well as surface-attached droplets (AG), will dominate the respective phases. Currently, the simulation of longer chains, aiming at the identification of all conformational phases and the quantitative analysis in the thermodynamic limit, is too challenging. Thus, a more detailed classification within the compact phases is left for future work.

C. Adsorption Parameters

The adsorption transition can be discussed best when looking at the distance of the center-of-mass of the polymer to the surface (Figure 11) and the mean number of surface contacts (Figures 12 and 13). As can be seen in Figure 11, for large temperatures and small values of ϵ_s, the polymer can move freely within the simulation box and the influence of the substrate is purely steric. Thus, the average center-of-mass distance $\langle z_{\mathrm{cm}}\rangle$ of the polymer above the surface is just half the height of the simulation box. On the other hand, for high ϵ_s values and low temperatures, the polymer favors surface contacts and the average center-of-mass distance converges to $\langle z_{\mathrm{cm}}\rangle \approx 0.858$, corresponding to the minimum-energy distance of the surface attraction potential for single-layer structures, and slightly larger valuesr for double-layer and globular structures.

One clearly identifies a quite sharp adsorption transition that divides the projection of $\langle z_{\mathrm{cm}}\rangle$ in Figure

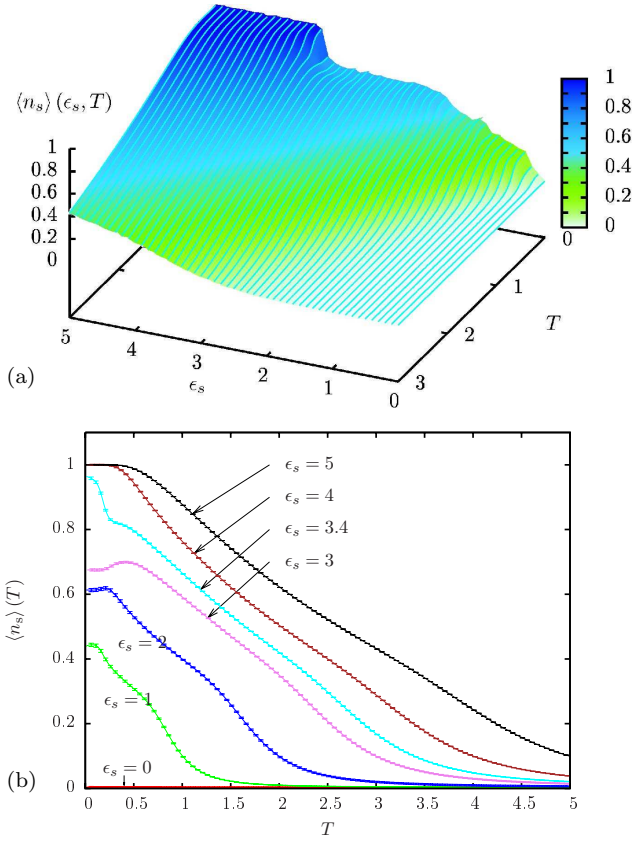

FIG. 13: (a) $\langle n_s\rangle$ of the 20mer. (b) $\langle n_s\rangle$ for different values of ϵ_s.

11a into an adsorbed (bright/green) regime and a desorbed (dark/blue) regime. This transition appears as a straight line in the phase diagram and is parametrized by $\epsilon_s \propto T$. Intuitively, this makes sense since at higher T the stronger Brownian fluctuations are more likely to overcome the surface attraction.

Consistently with our above discussion, $\langle z_{\rm cm}\rangle$ and $\mathrm{d}\langle z_{\rm cm}\rangle/\mathrm{d}T$ also reveal the low-temperature transitions between the adsorbed phases AC2a, AC2b, and AC1. for the detailed discussion of these adsorbed phases, we concentrate ourselves on the mean number of surface contacts $\langle n_s\rangle$ (Figs. 12, 13).

Unlike in simple-cubic lattice studies, where one finds $\langle n_s\rangle \approx 1$ for an l-layer structure [7], we find for double layer structures $\langle n_s\rangle > 1/2$. The reason is that most compact multilayer structures are cuboids on the lattice, whereas in our off-lattice study, "layered" conformations correspond to semispherical shapes, where, for optimization of the surface of the compact shape, the surface layer contains more monomers than the upper layer. Since this only regards the outer part of the layers, the difference is more pronounced the shorter the chain is.

In Figure 12, $\langle n_s\rangle$ is shown as a function of ϵ_s for small temperatures. $\langle n_s\rangle$ is a useful quantity to identify layering effects. Starting at high ϵ_s, for both chain lengths first $\langle n_s\rangle \approx 1$ until at the layering transition, $\langle n_s\rangle$ jumps to $\langle n_s\rangle \approx 0.69$ for $N = 13$ and to $\langle n_s\rangle \approx 0.65$ for $N = 20$.

Further jumps corresponding to further layering transitions are not observed. Instead, what follows is a plateau regime where the relative amount of monomers that cover the surface is rather constant. When the double-layer structure gets unstable at lower ϵ_s, $\langle n_s\rangle$ starts to decrease again. The conformations in AC and AC2a thus do not exhibit a pronounced number of surface contacts, and $\langle n_s\rangle$ varies with ϵ_s. Near $\epsilon_s \approx 0.2$, where the polymer desorbs, $\langle n_s\rangle$ converges rapidly to $\langle n_s\rangle = 0$ as $\epsilon_s \to 0$. To conclude, the single- to double-layer "layering transition" is a topological transition from 2D to 3D polymer conformations adsorbed at the substrate. The solvent-exposed part of the adsorbed compact polymer structure, which is not in direct contact with the substrate, reduces under poor solvent conditions the contact surface to the solvent. Because of the larger number of degrees of freedom for the off-lattice polymer, layered structures are not favored in this case. Thus, higher-order layering transitions are not identified in our analyses (which in part is also due to the short lengths of the chains) but are also not expected in pronounced form.

The observable left to discuss is the mean number of intrinsic contacts. It behaves very much like the radius of gyration, such that the projection of $\langle n_m\rangle$ onto the T-ϵ_s-plane is divided into a compact regime comprising AC, AG, AC2a, AC2b, DC, and DG and a regime of less compact conformations. This nicely confirms the results already obtained.

D. The Pseudophase Diagram

To summarize all the informations gained from the different observables, we construct the approximate boundaries of different regimes in the T-ϵ_s plane. The pseudophase diagram was already displayed in Figure 2 where the different pseudophases are denoted by the abbreviations explained in the previous subsection.

The pseudophases found are (for selected representative conformations see Figure 3):

- **DE** (desorbed expanded): Random-coil phase of the quasifree desorbed polymer.
- **DG** (desorbed globular): Globular phase of the desorbed chain.
- **DC** (desorbed compact): Maximally compact, spherically shaped crystalline structures dominate this desorption phase below the freezing-transition temperatue.
- **AE1** (adsorbed expanded single layer): Adsorbed phase of expanded, rather planar but little compact random-coil conformations.
- **AE2** (adsorbed expanded 3D conformations): Adsorbed, unstructured random-coil-like expanded conformations with typically more than half of the monomers in contact with the attractive substrate are favored in this pseudophase.

- **AC1** (adsorbed compact single layer): Phase of adsorbed circularly compact filmlike conformations.
- **AG** (adsorbed globular 3D conformations): Representative conformations are surface-attached globular conformations and look like drops on the surface.
- **AC2a** (adsorbed compact 3D conformations): Compact, semispherically shaped crystalline conformations dominate in this subphase.
- **AC2b** (adsorbed compact double layers): Subphase of adsorbed, compact double-layer conformations. The occupation of the surface layer is slightly larger than that of the other layer.

AC2a and AC2b are subphases in the regime of the phase diagram, where adsorbed compact and topologically three-dimensional conformations are dominant. Since pronounced layering transitions as observed in lattice-polymer studies are not expected here, the discriminations of AC2a and AC2b is likely to be irrelevant in the thermodynamic limit. However, AC2a,b differ qualitatively from the phase AC1 of topologically 2D polymer films and we thus expect that the transition between filmlike (AC1) and semispherical conformations (AC2) is of thermodynamic relevance.

For $N = 13$, where the maximally compact conformation is more stable due to the high symmetry of the icosahedral structure, we found an additional subphase:

- **AC** (adsorbed icosahedral compact conformations): Like DC, but polymers typically are in touch with the surface. As a clear individual subphase only observed for $N = 13$.

The transition lines in the pseudophase diagram (Figure 2) represent the best compromise of all quantities analyzed separately in our study. Only in the thermodynamic limit of infinitely long chains are most of the identified pseudophase transitions expected to occur at sharp values of the parameters ϵ_s and T for all observables. For finitely long chains, the transition lines still vary with chain length N and are not well defined due to the broad peaks that are slightly different for different observables (see Figure 14). Taking that into account, the pseudophase diagram gives a good qualitative overview of the behavior of polymers near attractive substrates in dependence of environmental parameters such as solvent quality and temperature. The locations of the phase boundaries should be considered as rough guidelines.

IV. COMPARISON WITH LATTICE RESULTS

Finally, we would like to compare our results discussed here with those obtained from a similar model on a simple-cubic (sc) lattice [16, 18].

The lattice polymer is modeled as a nongrafted interacting self-avoiding walk confined between two infinitely extended parallel planar walls. One wall is short-range

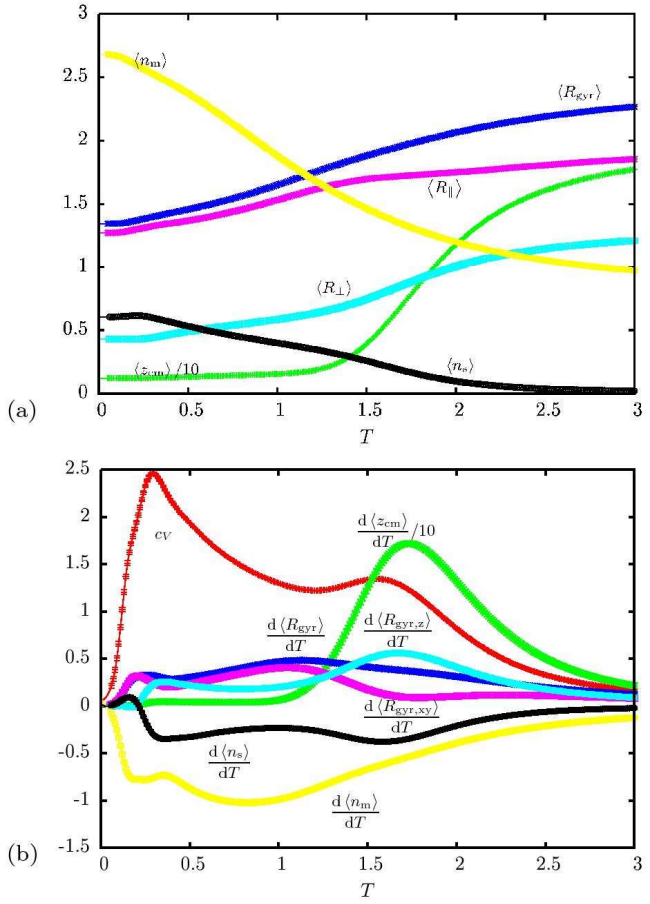

FIG. 14: (a) Temperature dependence of several observables for $\epsilon_s = 2$ and $N = 20$. (b) The derivative with respect to T of the same quantities.

attractive, and the other is purely sterical and prevents the polymer from escaping. The energy of the system is given by

$$E_{\mathrm{L}}\left(n_s^{\mathrm{L}}, n_m^{\mathrm{L}}\right) = -\epsilon_s^{\mathrm{L}} n_s^{\mathrm{L}} - \epsilon_m^{\mathrm{L}} n_m^{\mathrm{L}}, \tag{12}$$

where n_s^{L} is the number of nearest-neighbor monomer-substrate contacts, n_m^{L} is the number of nearest-neighbor but nonadjacent monomer-monomer contacts, and ϵ_s^{L} and ϵ_m^{L} are the respective contact energy scales. In refs [16] and [18] the contact density g_{n_s,n_m} was directly sampled by means of the contact-density chain-growth method, which is an extension of the multicanonical chain-growth method [36, 37]. The pseudophase diagram, parameterized by temperature and monomer-monomer interaction strengh was discussed mainly using the specific-heat profile. For a review see ref [38]. The surface-monomer attraction strength was fixed. With the contact density, the specific-heat profile can be calculated for fixed monomer-monomer interaction $\epsilon_m^{\mathrm{L}} = 1$, while varying the surface attraction parameter ϵ_s^{L} as it was done in the present off-lattice study. The resulting pseudophase diagram is depicted for a 179mer in Figure 15, where the parametrization chosen in ref [16] was

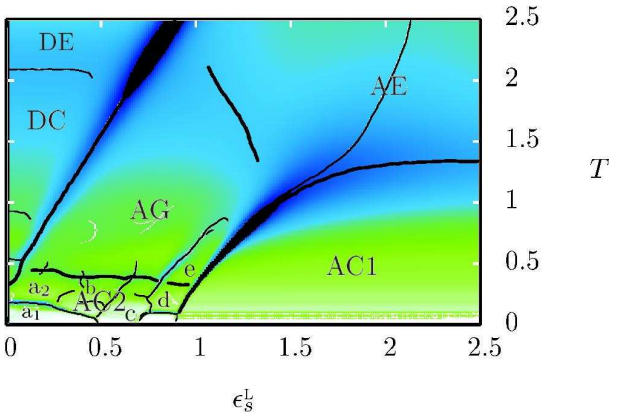

FIG. 15: Pseudophase diagram of a lattice polymer with 179 monomers[16], parametrized by the surface attraction strength, ϵ_s^{L}, and temperature, T. The color encodes the specific-heat profile; the darker the color, the larger its value.

rescaled in order to allow for a more direct comparison with the results of our off-lattice study. Denoting the energy and temperature from ref [16] with E' and T', respectively, the rescaling works as follows:

$$\begin{aligned} \frac{E'}{T'} = \frac{E_{\mathrm{L}}}{T} \quad &\Leftrightarrow \quad \frac{n_s^{\mathrm{L}} + s n_m^{\mathrm{L}}}{T'} = \frac{\epsilon_s^{\mathrm{L}} n_s^{\mathrm{L}} + n_m^{\mathrm{L}}}{T} \\ \Leftrightarrow T = \frac{T'}{s} \quad &\wedge \quad \epsilon_s^{\mathrm{L}} = \frac{1}{s}. \end{aligned} \tag{13}$$

Here, $s = \epsilon_m^{\mathrm{L}}/\epsilon_s^{\mathrm{L}}$ is the ratio of energy scales of intrinsic and surface contacts as introduced in ref [16]. It can be interpreted as a reciprocal solvent-quality parameter.

Certain similarities between the off-lattice (Figure 2) and the lattice pseudophase diagram (Figure 15) are obvious. For instance, the adsorption transition line is parametrized in both models by $\epsilon_s \propto T$. Different, however, is not only the slope, which depends on the system's geometry and energy scales, but also for the off-lattice model the extrapolation of the transition line seems to go through the origin $\epsilon_s = 0$ and $T = 0$, whereas there is an offset observed in the lattice-system analsis such that the extrapolated transition line roughly crosses $\epsilon_s^{\mathrm{L}} = 0.4$ and $T = 0$. We speculate that this might be due to the intrinsic cuboidal structure of the polymer conformation on the sc lattice that possess planar surfaces at low temperatures even in bulk. Unlike for off-lattice models, where a compact polymer attains a spherical shape, such a cuboidal conformation is likely to dock at a substrate without substantial conformational rearrangements. Here lies an important difference between lattice and off-lattice models. The off-lattice model provides, for sufficiently small surface attraction strengths, a competition between most compact spherical conformations that do not possess planar regions on the polymer surface and less compact conformations with planar regions that allow for more surface contacts but reduce the number of intrinsic contacts.

This also explains why a transition like the one observed for $N = 13$ between AC and AC2a, the wetting transition, is more difficult to observe in adsorption studies on regular lattices. On the other hand, AC2 conformations at low T and for ϵ_s between the adsorption and the single-double layering transitions can be observed in both models. Similarly in both models, there exists the AG pseudophase of surface-attached globules.

Whereas for the off-lattice model, apart from the wetting transition, there is only the transition from AC2a (semispherically shaped) to AC2b (double-layer structures), on the lattice AC2 comprises of a zoo of subphase transitions. These are higher-order layering transitions. Decreasing the surface attraction at low temperature, layer after layer is added until the number of layers is the same as in the most compact conformation. A lattice polymer has no other choice than forming layers in this regime. The layering transition from AC1 to AC2 is very sharp in both models. Also the shape of the transition region from topologically 2D adsorbed to 3D adsorbed conformations looks very similar. Interestingly, the $\epsilon_s^{\mathrm{L}}/\epsilon_m^{\mathrm{L}}$-ratio predicted for this transition in ref [7] agrees quite well with that observed in our off-lattice study. For low-energy conformations, it is argued that $l^{3/2} = (1 - \epsilon_s^{\mathrm{L}}/\epsilon_m^{\mathrm{L}})N^{1/2}$ on the square lattice. With $l = 1.5$ and $N = 179$ this gives $\epsilon_s^{\mathrm{L}}/\epsilon_m^{\mathrm{L}} = 0.914$ for the single- to double-layer transition, which is confirmed by Fig. 15. We re-expressed this argument for a triangular lattice, which describes the low-temperature conformations of our off-lattice model better, and obtain $l^{3/2} = 2(3 - \epsilon_s/\epsilon_m)N^{1/2}/3$ for low-energy configurations. This yields the larger ratio $\epsilon_s/\epsilon_m = 2.235\,(2.384)$ for $N = 13\,(20)$, which is due to the higher coordination number of this geometry. It is in good agreement with our simulation results for this transition. The higher coordination number also causes the different slopes of the respective adsorption transitions.

To summarize, we conclude that, in particular, the high-temperature pseudophases, DE, DC/DG, AG, and AE, nicely correspond to each other in both models. Noticeable qualitative deviations occur, as expected, in those regions of the pseudophase diagram where compact conformations are dominant.

V. SUMMARY

In this paper, we have constructed the pseudophase diagram of thermodynamic conformational phases of a single semiflexible homopolymer near an attractive substrate in dependence of the external parameters surface attraction strength and temperature.

For two polymer chains with $N = 13$ and $N = 20$ monomers, respectively, the canonical expectation values of several energetical and structural quantities and their thermal fluctuations were measured in multicanonical computer simulations over a broad range of surface

attraction strengths and temperatures. Conformational phases and phase boundaries and their location in the pseudophase diagram were identified in precise analyses of structural fluctuations and suitable adsorption parameters.

Although the computational expense to accurately explore such a broad parameter range restricted us to investigate rather short chains, we identified the following conformational pseudophases and pseudophase transitions:

- Crystalline structures in the regimes of compact phases. We identified maximally compact desorbed conformations in bulk (DC) or adsorbed at the substrate (AC), semispherical compact conformations (AC2a) that are distorted by the surface but not layered, double-layer conformation (AC2b), and single-layer conformations (AC1).
- Adsorbed conformations in the globular and expanded (random-coil) phases. Here, three conformational pseudophases were distinguished: unstructured 3D surface-attached globular conformations (AG), expanded dissolved but planar adsorbed conformations (AE1), and 3D expanded random-coil-like adsorbed conformations (AE2).
- Desorbed conformations. Compact conformations (DC) are separated by the freezing transition from globular conformations (DG). At even higher temperatures above the θ-transition, random-coil conformations are found (DE).

The sharpest pseudophase transition identified is the layering transition between single- and double-layer-structures. Higher-layer conformations were not found for these short chains. Unlike in recent studies on a simple-cubic lattice, where for weak surface attraction and positive self-attraction, layering transitions were observed until a maximally compact cubic structure is reached, off-lattice polymers favor maximally compact spherical conformation. Thus, we find the expected differences in the behavior of off-lattice and lattice polymers in phases, where compact adsorbed conformations dominate. For the majority of pseudophases, in particular those that are assumed to be relevant in the thermodynamic limit, we find, however, a nice qualitative coincidence. This similarity demonstrates the ability of such simple coarse-grained models to capture the general adsorption behavior of polymers near attractive surfaces. The increasing experimental and technological capabilities should allow not only for the experimental verification of the described thermodynamic phases but also for a detection of the pseudophases of finite polymers. Since polymers are naturally of finite length, this problem is one of real physical interest.

VI. ACKNOWLEDGEMENTS

This work is partially supported by the DFG (German Science Foundation) under Grant Nos. JA 483/24-1/2 and the Leipzig Graduate School of Excellence "BuildMoNa". Support by a NIC supercomputer time grant (No. hlz11) of the Forschungszentrum Jülich is acknowledged.

[1] F. Kuhner, M. Erdmann, and H. E. Gaub, Phys. Rev. Lett. **97**, 218301 (2006).
[2] K. Goede, P. Busch, and M. Grundmann, Nano Lett. **4**, 2115 (2004).
[3] D. E. Smith, S. J. Tans, S. B. Smith, S. Grimes, D. L. Anderson, and C. Bustamante, Nature **413**, 748 (2001).
[4] K. Kegler, M. Salomo, and F. Kremer, Phys. Rev. Lett. **98**, 058304 (2007).
[5] W. Paul, T. Strauch, F. Rampf, and K. Binder, Phys. Rev. E **75**, 060801(R) (2007).
[6] T. Vogel, M. Bachmann, and W. Janke, Phys. Rev. E **76**, 061803 (2007).
[7] J. Krawczyk, A. L. Owczarek, T. Prellberg, and A. Rechnitzer, Europhys. Lett. **70**, 726 (2005).
[8] J. Luettmer-Strathmann, F. Rampf, W. Paul, and K. Binder, J. Chem. Phys. **128**, 064903 (2008).
[9] E. Eisenriegler, K. Kremer, and K. Binder, J. Chem. Phys. **77**, 6296 (1982).
[10] Z. Usatenko, J. Stat. Mech., P03009 (2006).
[11] J. Forsman and C. E. Woodward, Phys. Rev. Lett. **94**, 118301 (2005).
[12] R. Rajesh, D. Dhar, D. Giri, S. Kumar, and Y. Singh, Phys. Rev. E **65**, 056124 (2002).
[13] E. Eisenriegler, *Polymers near Surfaces: Conformation Properties and Relation to Critical Phenomena* (World Scientific, Singapore, 1993).
[14] S. Metzger, M. Müller, and K. Binder, J. Chem. Phys. **118**, 8489 (2003).
[15] P. Schravendijk, L. Ghiringhelli, L. Site, and N. van der Vegt, J. Phys. Chem. C **111**, 2631 (2007).
[16] M. Bachmann and W. Janke, Phys. Rev. E **73**, 041802 (2006).
[17] N. Gupta and A. Irbäck, J. Chem. Phys. **120**, 3983 (2004).
[18] M. Bachmann and W. Janke, Phys. Rev. Lett. **95**, 058102 (2005).
[19] T. Vrbová and S. G. Whittington, J. Phys. A **31**, 3989 (1998).
[20] R. Hegger and P. Grassberger, J. Phys. A **27**, 4069 (1994).
[21] M. Bachmann and W. Janke, Phys. Rev. E **73**, 020901(R) (2006).
[22] F. Celestini, T. Frisch, and X. Oyharcabal, Phys. Rev. E **70**, 012801 (2004).
[23] Y. Singh, D. Giri, and S. Kumar, J. Phys. A **34**, L67 (2001).
[24] N. Källrot and P. Linse, Macromolecules **40**, 4669 (2007).
[25] F. Stillinger, T. Head-Gordon, and C. Hirshfeld, Phys.

Rev. E **48**, 1469 (1993).
[26] F. Stillinger and T. Head-Gordon, Phys. Rev. E **52**, 2872 (1995).
[27] S. Schnabel, M. Bachmann, and W. Janke, Phys. Rev. Lett. **98**, 048103 (2007).
[28] S. Schnabel, M. Bachmann, and W. Janke, J. Chem. Phys. **126**, 105102 (2007).
[29] W. A. Steele, Surf. Sci. **36**, 317 (1973).
[30] R. Hentschke, Macromol. Theory Simul. **6**, 287 (1997).
[31] B. Berg and T. Neuhaus, Phys. Lett. B **267**, 249 (1991).
[32] W. Janke, Physica A **254**, 164 (1998).
[33] B. Berg, Fields Inst. Commun. **26**, 1 (2000).
[34] S. Schnabel, T. Vogel, M. Bachmann, and W. Janke, to be published (2008).
[35] A. L. Mackay, Acta Cryst. **15**, 916 (1962).
[36] M. Bachmann and W. Janke, Phys. Rev. Lett. **91**, 208105 (2003).
[37] T. Prellberg and J. Krawczyk, Phys. Rev. Lett. **92**, 120602 (2004).
[38] M. Bachmann and W. Janke, in: *Rugged Free Energy Landscapes: Common Computational Approaches to Spin Glasses, Structural Glasses and Biological Macromolecules*, edited by W. Janke, Lect. Notes Phys. **736** (Springer, Berlin, 2008), pp. 203–246.